JOURNAL OF CHEMICAL & ENGINEERING DATA

ARTICLE

pubs.acs.org/jced

Vapor−Liquid Equilibria Measurements of the Methane + Pentane and Methane + Hexane Systems at Temperatures from (173 to 330) K and Pressures to 14 MPa

Mohamed E. Kandil,[†] Markus J. Thoma,[‡] Tauqir Syed,[†] Jerry Guo,[†] Brendan F. Graham,[†] Kenneth N. Marsh,[†] Stanley H. Huang,[§] and Eric F. May[†,*]

[†]Centre for Energy, School of Mechanical & Chemical Engineering, University of Western Australia, Crawley, WA, Australia 6009

[‡]Laboratory of Plant and Process Design, Technical University Munich, 85748 Garching, Bavaria, Germany

[§]Chevron Energy Technology Company, Houston, Texas 77002, United States

ABSTRACT: New *pTxy* data are reported for methane + pentane and methane + hexane at pressures up to 14 MPa over the temperature range (173 to 333) K using a custom-built vapor−liquid equilibria apparatus. For methane (1) + pentane (2), a mixture with overall mole fraction $z_2 \approx 0.02$ was prepared gravimetrically, and measurements were performed along an isochoric pathway. For the methane (1) + hexane (3) mixture, liquid hexane was pumped into the evacuated cell using an HPLC pump, and then after the addition of methane, isothermal measurements were made at 11 temperatures. Two liquid phases were observed close to the bubble point in the methane + hexane mixture at (183.15 and 233.15) K at pressures of (3.31 and 12.99) MPa, respectively. Our data are compared with previous literature data and with the predictions of the Groupe European de Recherche Gaziere (GERG-2004 XT08) multiparameter equation of state (EOS) and the Peng−Robinson and Advanced Peng−Robinson cubic equations of state implemented in commercial process simulation software. The differences from the GERG-2004 EOS in the liquid phase mole fraction x_1 were up to 0.1 for methane + pentane and up to 0.3 for methane + hexane. The systematic increase in the deviations with pressure, at constant temperature, is clear evidence of the need for tuning of the EOS parameters, especially at high pressure. The differences are smaller for the Peng−Robinson and the Advanced Peng−Robinson EOS; however, all three EOS failed to predict the second liquid phase in methane + hexane. Our data agree with the x_1 values reported by Chen et al. (*J. Chem. Eng. Data* **1976**, *21*, 213−219) for the appearance of a second liquid phase.

INTRODUCTION

The construction and operation of a liquefied natural gas (LNG) facility requires significant capital expenditure. For such a multibillion dollar investment, optimized plant and process design is crucial. A major process operation in an LNG plant is the so-called scrub column where the liquefied petroleum gases (LPG) and the heavier hydrocarbon liquids are separated from the stream heading to the main cryogenic heat exchanger to avoid potential freezing in further downstream processing. Often simulator predictions for the product streams of these columns deviate significantly from actual product streams observed in operating plant data; those predictions have been shown to have an unexpected sensitivity to the selected simulation software and the selected property package.[1] This also applies to different equations of state within the same simulator, such as the Peng−Robinson[2] and Soave−Redlich−Kwong[3] equations of state (EOS) implemented in AspenTech HYSYS,[4] which according to the software manual should give nominally equivalent results, for near-ideal (hydrocarbon) systems at temperatures greater than 130 K and pressures below 35 MPa.[5]

The GERG-2004 EOS[6] for natural gases and other mixtures, released in 2007, and its extension GERG-2004 XT08 released in 2008 to cover three additional components are significant steps forward in the description of the thermodynamic properties of natural gas mixtures. However, the developers of this EOS, Kunz et al.,[6] have identified that the VLE data situation for mixtures of natural gas components is unsatisfactory, and there are not enough high-quality thermodynamic data to reliably represent the LNG mixtures at high-pressure and cryogenic conditions. In our previous paper[8] we reported the construction of a cryogenic apparatus for VLE measurements at high pressure and also reported *pTxy* measurements on methane + 2-methylpropane (isobutane). In this paper *pTxy* measurements are reported for the two binary systems, methane + pentane and methane + hexane, and the results are compared with three equations of state: GERG-2004 XT08 EOS as implemented in Microsoft Excel, the Peng−Robinson (PR) EOS as implemented in the software Aspen HYSYS, and the Advanced Peng−Robinson (APR) EOS as implemented in the software VMGSim.[7]

APPARATUS AND MATERIALS

The experimental apparatus and technique have been described in detail previously,[8] and only major variations are reported here. For measurements on methane + hexane an additional heating element was fitted onto the cell lid to minimize the thermal gradient observed during the measurements on

Special Issue: Kenneth N. Marsh Festschrift

Received: January 26, 2011
Accepted: February 23, 2011
Published: March 21, 2011

methane + pentane and previously identified in our work on methane + 2-methylpropane,[8] where the temperature difference between the top and bottom of the cell reached 0.6 K. In addition, the stepper motor used to stir the liquid nitrogen boil-off vapor in the Dewar was replaced with a more powerful overhead stirrer: the new motor, located outside the Dewar, drove a shaft and a fan located in the Dewar. These two improvements allowed the control of the thermal gradient between the top and bottom of the cell to be < 0.02 K. These three improvements were made after the methane + pentane measurements were completed.

For methane + hexane it was not possible to prepare a single-phase gas mixture of the required hexane mole fraction at room temperature. Mixtures were instead prepared by connecting a high-pressure liquid chromatograph pump (HPLC) containing hexane to the system and injecting it directly into the equilibrium cell. Methane was then added and mixed to produce the system pressure close to that desired.

The sampling method was also improved, for measurements of both binary systems, by adding two bypass valves on the lines connecting the VLE cell to the GC. These valves were used to discard the first few samples taken from the cell, which were unrepresentative of the equilibrium because they contained fluid trapped for a significant time in the capillaries. Previously, multiple samples were also taken, but as described in ref 8, all these samples went through the column and into the GC detectors; the GC method was adjusted to avoid coelution of the peaks from multiple samples, and only the last several samples were included in the analysis. However, we found that the viability of this method decreased as the boiling point of the heavy component in the mixture increased and would become completely unviable for measurements of multicomponent mixtures. In the new arrangement, the rotary bypass valves were initially set to flush the acquired samples to waste. After a fixed amount of time during which about 5 to 10 samples from the cell were flushed, the valves would automatically change position to direct the final sample onto the GC column. The GC response to the single, representative sample was recorded and the procedure repeated, about 5 to 8 times, to obtain an average and standard deviation for the composition of each phase. The total amount of material removed from the cell was comparable with but slightly more than in Kandil et al.;[8] any decrease in cell pressure observed was much smaller than the uncertainty of the pressure measurement.

Ultrahigh purity methane was supplied by Air Liquide with specified $x > 0.99995$, and principal mole fraction impurities were reported by the supplier as less than $25 \cdot 10^{-6}$ air, $15 \cdot 10^{-6}$ C_2H_6, $5 \cdot 10^{-6}$ H_2O, $5 \cdot 10^{-6}$ other hydrocarbons, and $1 \cdot 10^{-6}$ CO_2. Analytical grade pentane and hexane were supplied by Fluka, with $x > 0.99$, and principal mole fraction impurities were reported by the supplier as $< 1 \cdot 10^{-6}$ higher-boiling point impurities in pentane and $< 1 \cdot 10^{-4}$ H_2O in hexane.

CALIBRATION OF THE GC DETECTORS

To enable quantitative VLE measurements with a rigorous uncertainty assessment, we calibrated extensively the two flame ionization detectors (FIDs) of the GC. The calibration was conducted to determine the response factors, κ_i, of the FIDs for the three compounds methane ($i = 1$), pentane ($i = 2$), and hexane ($i = 3$), defined via the equation

$$A_i = \kappa_i n_i \tag{1}$$

Table 1. Calibration Results for the GC's Flame Ionization Detectors[a]

	methane (1)	pentane (2)	hexane (3)
		FID-L	
$\min(A_i)/(10^6$ counts)	0.03	0.16	0.12
$\max(A_i)/(10^6$ counts)	157.90	19.93	19.69
$\langle\kappa_i\rangle/(10^{13}$ counts/mol)	3.65	16.55	19.98
$u(\langle\kappa_i\rangle)/(10^{13}$ counts/mol)	0.20	1.18	1.45
$\langle\kappa_i/\kappa_1\rangle$	1	4.68	5.57
$u(\langle\kappa_i/\kappa_1\rangle)$		0.09	0.13
		FID-V	
$\min(A_i)/(10^6$ counts)	0.04	0.17	0.11
$\max(A_i)/(10^6$ counts)	70.80	3.98	4.24
$\langle\kappa_i\rangle/(10^{13}$ counts/mol)	3.59	16.91	20.05
$u(\langle\kappa_i\rangle)/(10^{13}$ counts/mol)	0.21	1.27	1.71
$\langle\kappa_i/\kappa_1\rangle$		4.73	5.61
$u(\langle\kappa_i/\kappa_1\rangle)$		0.13	0.21

[a] The angled brackets denote an average over all measurements.

Here n_i is the number of moles of component i measured at the detector, and A_i is the integrated detector response measured with the GC for component i. The instantaneous detector response is an electronic signal commonly measured in picoamperes or nanovolts depending on the GC's manufacturer; this signal is integrated with respect to time over a certain range to give the A_i, the units of which are commonly referred to as "counts". The mole fraction composition, z_i, of a given N component mixture analyzed with the GC can be determined from the measured ratios (A_i/A_j) by solving the system of equations

$$\left(\frac{z_i}{z_1}\right) = \left(\frac{A_i}{A_1}\right)\left(\frac{\kappa_1}{\kappa_i}\right) \tag{2a}$$

$$z_1 = 1 - \sum_{i=2}^{N} z_i \tag{2b}$$

where $i = 1$ would normally be taken as the mixture component with the largest integrated detector response, which is usually methane for natural gas mixtures. In the case of a binary mixture eq 2 simplifies to

$$z_2 = \frac{(A_2/A_1)}{(\kappa_2/\kappa_1) + (A_2/A_1)} \tag{3}$$

It is apparent from eq 2a that knowing the ratios (κ_i/κ_j) is sufficient for a given detector, and furthermore, estimating the uncertainties of those ratios is essential for the uncertainty analysis of the measured composition. A skilled operator can usually measure the ratios (A_i/A_j) with a relative precision of between 0.1 % and 1 % if the sampling and injection process is straightforward. Thus, if a gravimetrically prepared mixture is used to calibrate the detectors the ratios (κ_i/κ_j) can be determined directly from eq 2a. Determining the absolute values of the detector response coefficients is more difficult because it requires the number of moles of a component reaching the detector to be estimated reliably. However, knowledge of the κ_i can be helpful in estimating the number of moles being extracted from the VLE cell, for example, to ensure that a representative sample has been obtained.

In this work we determined the ratios (κ_2/κ_1), (κ_3/κ_1), and (κ_3/κ_2) from measurements of two gravimetrically prepared

Table 2. Measured Phase Compositions for Methane (1) + Pentane (2)[a]. The Data Point at 173 K May Correspond to a VLLE Condition

T	$u(T)$	p	$u(p)$						
K	K	MPa	MPa	x_1	$u(x_1)$	$u_c(x_1)$	y_2	$u(y_2)$	$u_c(y_2)$
243.31	0.19	7.943	0.04	0.514	0.005	0.009	0.0098	0.0003	0.0003
233.26	0.12	7.273	0.04	0.532	0.005	0.009	0.0068	0.0002	0.0002
223.28	0.14	6.594	0.03	0.557	0.005	0.010	0.0048	0.0002	0.0002
213.33	0.18	5.896	0.03	0.594	0.005	0.012	0.0034	0.0001	0.0002
203.42	0.27	5.183	0.03	0.668	0.004	0.013	0.0020	0.0001	0.0001
188.43	0.28	3.937	0.02	0.938	0.001	0.015	0.0006	0.0000	0.0001
173.43	0.29	2.417	0.01	0.996	0.000	0.018	0.0001	0.0000	0.0001
223.31	0.16	6.444	0.03	0.536	0.005	0.010	0.0043	0.0001	0.0001
243.21	0.07	7.641	0.04	0.506	0.005	0.009	0.0094	0.0003	0.0003

[a] $u(q)$ represents the uncertainty in the quantity q, as discussed in the text, while the combined uncertainty $u_c(x_1)$ and $u_c(y_2)$ includes the effect of the propagated temperature and pressure uncertainties on the measured compositions combined with the uncertainties of the composition measurements.

mixtures. These mixture calibration measurements were supplemented with pure fluid calibration measurements to estimate the absolute values of κ_1, κ_2, and κ_3 over a wider range of integrated detector response. One of the calibration mixtures was a commercially supplied dilute helium reference mixture with $z_1 \cong z_2 \cong z_3 \cong (1000 \pm 2) \cdot 10^{-3}$, while the other was a ternary mixture prepared gravimetrically in our laboratory with $z_1 = 0.9835 \pm 0.0007$, $z_2 = 0.0110 \pm 0.0006$, and $z_3 = 0.0055 \pm 0.0004$ using a procedure similar to that described in the Methods and Analysis section. A summary of the results of the calibration are listed in Table 1, where FID-L and FID-V are the flame ionization detectors for the nominally liquid and vapor phases, respectively. These ratios were used to determine the values of x_2, y_2, x_3, and y_3 listed in Tables 2 and 3.

The two FID detectors on the GC were calibrated simultaneously using either an in-built sampling manifold designed for gaseous calibrants (helium mixture, ternary mixture, pure methane) or an in-built sampling manifold for liquid calibrants (pentane, hexane, and gravimetrically prepared solutions of pentane or hexane in methanol). The liquid sampling manifold consisted of a four-port rotary valve connecting an internal sample loop of 0.135 μL either to a fill line or to the GC injector. With the rotary valve in the former position, an HPLC pump was used to flow the liquid calibrant through the internal 0.135 μL loop to waste. After pumping a sufficient volume through the internal loop, the flow was stopped and the rotary valve actuated so that the liquid calibrant was driven from the internal loop into the GC injector by the carrier gas. The internal 0.135 μL loop could only be connected to one of the detectors, FID-L, so only this detector was calibrated with liquid-phase samples.

The sampling manifold for gaseous calibrants consisted of two, six-port rotary valves and two external sampling loops connected in series when the valves were in the fill position. Each of the external sampling loops could be removed and replaced with another loop of a different volume. Loops with volumes ranging from (25 to 5000) μL were connected to determine the response of each detector over a wide range of injected amounts. The cylinder containing the gaseous calibrant was connected to the manifold, and the gas was allowed to

Table 3. Measured Phase Compositions for Methane (1) + Hexane (3)[b]. The Data Points near (233 K, 12.9 MPa) and (183 K, 3.3 MPa) May Correspond to a VLLE Condition

T	p	$u(p)$						
K	MPa	MPa	x_1	$u(x_1)$	$u_c(x_1)$	y_3	$u(y_3)$	$u_c(y_3)$
333.15	2.63	0.01	0.123	0.003	0.005	0.0350	0.0013	0.0013
333.15	4.57	0.02	0.196	0.004	0.006	0.0289	0.0010	0.0010
333.15	7.37	0.04	0.295	0.005	0.007	0.0377	0.0015	0.0015
333.15	10.15	0.05	0.386	0.006	0.007	0.0375	0.0013	0.0013
333.15	13.77	0.07	0.502	0.006	0.008	0.0390	0.0014	0.0014
318.15	2.43	0.01	0.122	0.003	0.006	0.0283	0.0010	0.0010
318.15	5.11	0.03	0.228	0.004	0.007	0.0228	0.0008	0.0008
318.15	7.75	0.04	0.323	0.005	0.007	0.0244	0.0009	0.0009
318.15	11.18	0.06	0.429	0.006	0.008	0.0321	0.0011	0.0011
318.15	14.21	0.07	0.529	0.006	0.008	0.0217	0.0010	0.0010
303.15	2.07	0.01	0.112	0.002	0.006	0.0168	0.0006	0.0006
303.15	5.87	0.03	0.267	0.005	0.008	0.0199	0.0008	0.0008
303.15	8.39	0.04	0.353	0.006	0.008	0.0182	0.0007	0.0007
303.15	11.07	0.06	0.445	0.006	0.008	0.0229	0.0008	0.0008
303.15	14.19	0.07	0.546	0.006	0.009	0.0170	0.0007	0.0007
288.15	2.35	0.01	0.136	0.003	0.007	0.0097	0.0003	0.0004
288.15	4.20	0.02	0.221	0.004	0.008	0.0126	0.0008	0.0008
288.15	6.22	0.03	0.299	0.005	0.009	0.0137	0.0010	0.0010
288.15	8.93	0.04	0.400	0.006	0.009	0.0130	0.0005	0.0005
288.15	12.32	0.06	0.516	0.007	0.009	0.0222	0.0008	0.0008
273.15	2.29	0.01	0.142	0.003	0.008	0.0037	0.0003	0.0003
273.15	4.19	0.02	0.233	0.005	0.009	0.0039	0.0001	0.0002
273.15	6.03	0.03	0.306	0.013	0.015	0.0048	0.0006	0.0007
273.15	6.11	0.03	0.315	0.005	0.009	0.0042	0.0002	0.0002
273.15	8.13	0.04	0.401	0.006	0.010	0.0056	0.0002	0.0003
273.15	10.85	0.05	0.498	0.007	0.010	0.0109	0.0004	0.0004
273.15	14.23	0.07	0.611	0.006	0.009	0.0270	0.0009	0.0010
253.15	2.04	0.00	0.152	0.003	0.009	0.0033	0.0002	0.0002
253.15	3.97	0.00	0.259	0.005	0.010	0.0020	0.0001	0.0002
253.15	6.15	0.00	0.361	0.006	0.010	0.0028	0.0001	0.0002
253.15	9.13	0.00	0.477	0.006	0.011	0.0056	0.0002	0.0003
253.15	11.87	0.00	0.575	0.006	0.011	0.0057	0.0002	0.0003
233.15	1.98	0.01	0.182	0.004	0.010	0.0009	0.0001	0.0002
233.15	4.06	0.02	0.314	0.005	0.011	0.0011	0.0001	0.0002
233.15	5.91	0.03	0.415	0.006	0.012	0.0018	0.0001	0.0002
233.15	7.99	0.04	0.517	0.006	0.012	0.0037	0.0001	0.0002
233.15	10.36	0.05	0.647	0.011	0.015	0.0105	0.0004	0.0004
233.15	12.87	0.06	0.959	0.001	0.010	0.0250	0.0013	0.0013
233.15	12.99	0.06	0.954	0.001	0.010			
233.15	12.99	0.06	0.957	0.001	0.010			
213.15	2.16	0.01	0.252	0.005	0.012	0.0004	0.0000	0.0002
213.15	4.08	0.02	0.415	0.006	0.013	0.0007	0.0001	0.0003
213.15	6.40	0.03	0.592	0.006	0.012	0.0017	0.0001	0.0003
203.15	1.43	0.01	0.214	0.004	0.012	0.0006	0.0001	0.0003
203.15	3.03	0.02	0.382	0.006	0.013	0.0005	0.0000	0.0003
203.15	4.59	0.02	0.546	0.008	0.014	0.0005	0.0000	0.0003
203.15	6.13	0.03	0.677	0.011	0.016	0.0015	0.0001	0.0003
193.15	2.06	0.01	0.352	0.013	0.018	0.0002	0.0000	0.0003
193.15	3.26	0.02	0.519	0.008	0.015	0.0003	0.0000	0.0003
193.15	3.39	0.02	0.535	0.006	0.014	0.0004	0.0001	0.0003

dx.doi.org/10.1021/je200101x |J. Chem. Eng. Data 2011, 56, 4301–4309

Table 3. Continued

T	p	$u(p)$						
K	MPa	MPa	x_1	$u(x_1)$	$u_c(x_1)$	y_3	$u(y_3)$	$u_c(y_3)$
193.15	4.88	0.02	0.714	0.005	0.013	0.0009	0.0002	0.0004
193.15	4.94	0.02	0.707	0.006	0.013	0.0021	0.0007	0.0007
183.15	1.86	0.01	0.413	0.009	0.015	0.0002	0.0000	0.0003
183.15	2.51	0.01	0.552	0.007	0.015	0.0003	0.0000	0.0003
183.15	3.03	0.02	0.693	0.006	0.014	0.0002	0.0000	0.0003
183.15	3.04	0.02	0.698	0.007	0.015	0.0009	0.0003	0.0004
183.15	3.31	0.02	0.955	0.002	0.013	0.0002	0.0000	0.0003

[b] The vapor-phase samples acquired at (233.15 K, 12.99 MPa) did not give repeatable values of y_3 and hence were omitted.

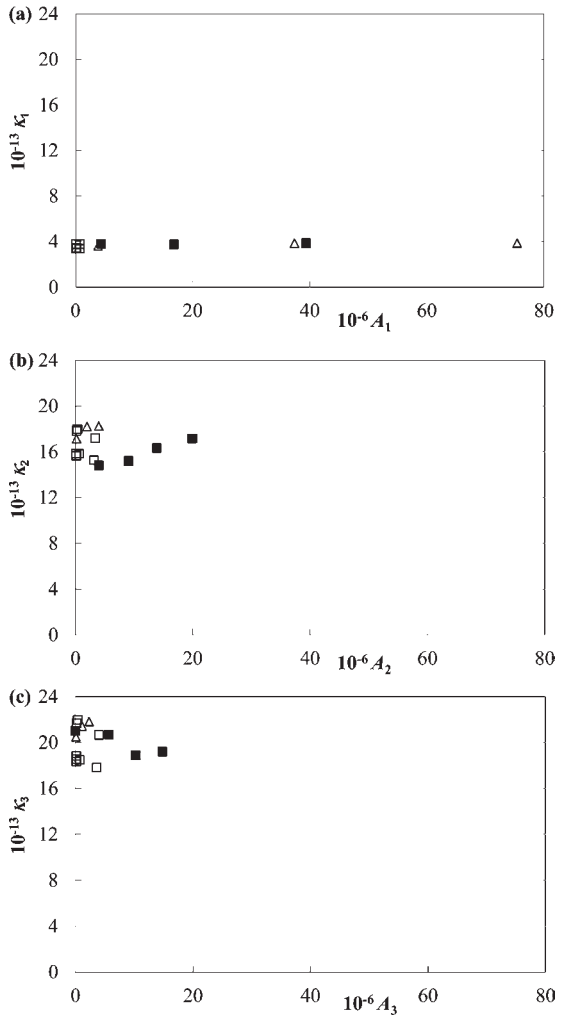

Figure 1. Absolute response coefficients, κ_i (counts per mole), against detector response A_i (counts) for FID-L for (a) methane (1), (b) pentane (2), and (c) hexane (3) determined by the calibration experiments with gravimetric mixtures and pure fluids. □, dilute helium mixture; ■, pure fluid or liquid solution; △, ternary mixture.

flow through both loops to waste. The gas flow rate was controlled by adjusting a manual flow meter connected at the end of the manifold.

The volumes of the external loops were measured prior to the GC detector calibrations by filling them with water, weighing them accurately, drying them in an oven, and repeating several times. The

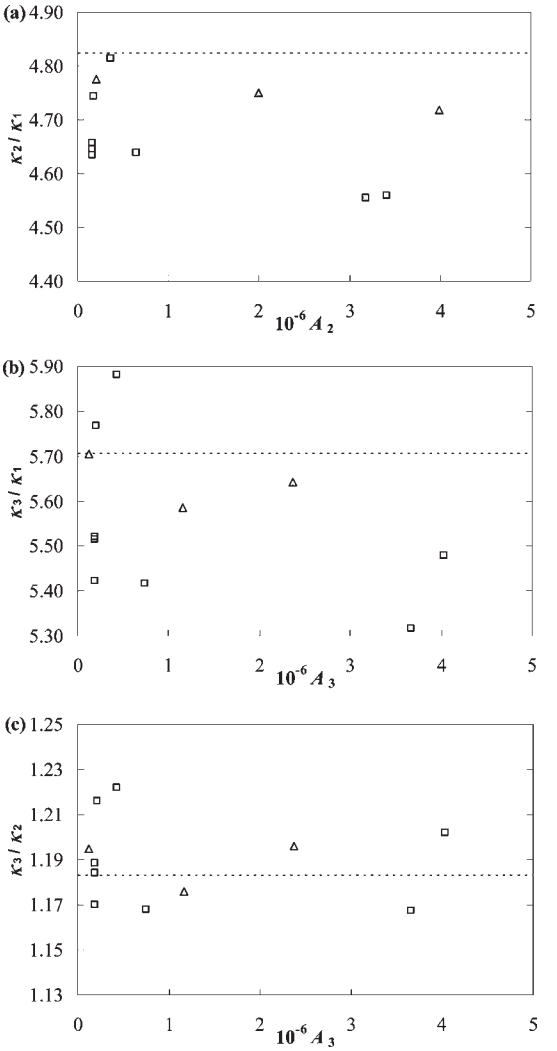

Figure 2. Response coefficient ratios, (κ_i/κ_j), for FID-L for (a) methane (1) and pentane (2), (b) methane and hexane (3), and (c) pentane and hexane determined by the calibration experiments with gravimetric gas mixtures: □, dilute helium mixture; △, ternary mixture and the dashed line, ----, represents the values derived from Dietz.[9]

internal loop on the liquid sampling manifold wasin fact an etching on the valve rotor face supplied by the GC manufacturer that could not be modified. To determine its actual volume (the manufacturer reported a nominal value of 0.2 μL) the internal loop was filled with methane at ambient conditions, and the response of FID-L was measured. This response was compared with the FID response obtained by filling the 250 μL external loop with methane: the ratio of the measured integrated detector responses was 1845, which was assumed to be equal to the volume ratio of the two loops.

The temperatures of the gas in the loops was measured with thermometers glued onto their exterior, and the pressure in the loops upon injection was taken to be atmospheric (hence the need to stop the flow prior to injection). The number of moles injected was estimated by combining the loop volume with the fluid's molar density calculated with an equation of state from the estimated temperature and pressure. Uncertainties in the estimated temperature due to inadequate temperature control of the gas and/or thermal gradients along the loops are reasons why determining accurately the absolute detector response factors is difficult.

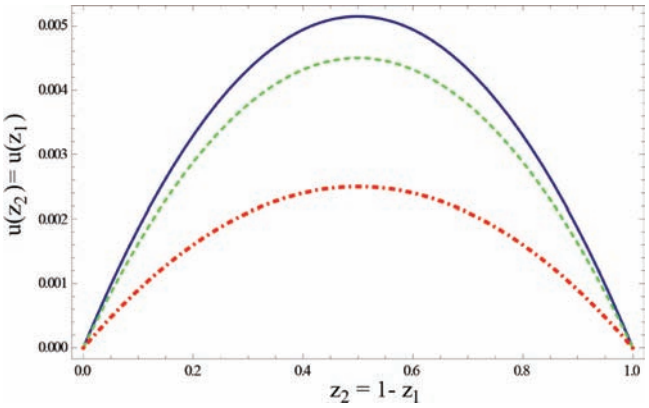

Figure 3. Simulated contributions to the uncertainty in the pentane mole fraction, $u(z_2)$, determined for a methane (1) + pentane (2) binary using eq 3 with $(\kappa_2/\kappa_1) = 4.67$ and relative uncertainties $u_r(\kappa_2/\kappa_1) = 0.018$ and $u_r(A_2/A_1) = 0.01$: dot-dashed line, $u_r(A_2/A_1)$ contribution; dashed line, $u_r(\kappa_2/\kappa_1)$ contribution; solid line, total uncertainty.

The value of n_i in eq 1 was calculated by dividing the number of moles in the sample loop by the injector split ratio, which was usually 10 to 1, and multiplying by the component's mole fraction if the injected sample was a gravimetrically prepared mixture. The repeatability and stability of the flow controller used by the GC to set this ratio also limits the uncertainty with which n_i can be estimated. Generally the electronic gain of each FID was set to maximum; however, in some cases it was reduced to ensure the signal size remained within the instrument's range. In such cases the effect of the electronic gain was incorporated into the analysis to determine an equivalent detector response (area) at maximum detector sensitivity.

Figure 1 shows the values of κ_i for the FID-L detector as a function of the A_i for each component. The responses for FID-V were similar but not identical. While linear regression of eq 1 to the data could be used to determine the κ_i, such an approach has an implicit heavy weighting on the point with the highest measured A_i. An equal weighting of all points is achieved by calculating the $\kappa_i = A_i/n_i$ for each point and then averaging over them all. For the data shown there is no evidence of detector nonlinearity for $A_i < 10^8$; the saturation of the detector response was observed when loops with volumes larger than 1000 μL were filled with the ternary mixture or pure methane, giving $A_1 > 1.4 \cdot 10^8$ counts. Rather, the dominant feature in the observed κ_i values is their scatter, which in relative terms ranged from 6 % for methane to 8% for hexane. Given that for each data point the value of A_i was determined from an average of three injections with a relative standard deviation of less than 1 %, we attribute the additional scatter to the limited repeatability of injections made over several weeks due to sample thermalization, temperature stability of the manifold injector lines, and injector split flow control.

Figure 2 shows the ratios (κ_2/κ_1), (κ_3/κ_1), and (κ_3/κ_2) plotted against either A_2 or A_3 for the two calibration gas mixtures. The relative scatter in each of the ratios is reduced by a factor of between 2 and 5 in comparison with the absolute detector responses, with relative standard deviations of 1.8 %, 3.0 %, and 1.6 %, respectively. It is apparent that the common-mode suppression of scatter was least prevalent for methane and hexane; the same value of (κ_3/κ_1) can be obtained from the ratios (κ_2/κ_1) and (κ_3/κ_2) with a relative standard uncertainty of 2.4 %. Figure 2 also shows that the measured values of (κ_3/κ_1), (κ_3/κ_1), and (κ_3/κ_2) are consistent with those estimated from the detector response factors tabulated by Dietz,[9] who also reported "a precision of about ± 3 %" (original wording).

Inspection of eq 3 indicates that there are two sources of uncertainty in the determination of a binary mixture's mole fraction composition arising from the GC measurement: a calibration uncertainty of about (1 to 3) % in (κ_i/κ_j) and the uncertainty in the measured area ratios (A_i/A_j), which can be attributed to the repeatability of sampling and injection and under favorable circumstances ranges from (0.1 to 1) %. To illustrate the minimum achievable uncertainties $u(z_1) = u(z_2)$ for a binary mixture, Figure 3 shows a simulated estimate of the two contributions for the measurement of methane + pentane mixtures using values determined for FID-L and assuming a relative uncertainty in the measured ratio of $u_r(A_2/A_1) = 1$ %. This value is about the same or larger than the level of repeatability in (A_2/A_1) achieved during the methane (1) + pentane (2) VLE measurements. Contributions due to uncertainty in the temperature and pressure of the system are not shown here, although they are considered below. It is apparent that both contributions to $u(z_2)$ are roughly quadratic with a maximum at $z_2 = 0.5$ and that the calibration uncertainty dominates for almost all values of z_2. It is clear that detector calibration uncertainties are the principal limitation of GC-based VLE measurements.

METHODS AND ANALYSIS

The methane (1) + pentane (2) single-phase mixture was prepared gravimetrically using a high-pressure, 300 cm^3 sample cylinder and 1100 g electronic balance with a 0.001 g resolution. A double-ended cylinder, containing a stainless steel ball, was sealed with a valve at one end and a threaded blank plug at the other, and then evacuated and weighed. After weighing, the cylinder was purged with 1 bar of N_2 gas before the threaded plug was removed, and liquid pentane was loaded using a syringe. The plug was replaced, and the cylinder was then placed in liquid nitrogen and re-evacuated to remove the gas inside. The sample cylinder was reheated to ambient temperature and then cooled again with liquid nitrogen and evacuated further; this precaution was taken in case any gas had been trapped beneath the frozen pentane during the first cycle. The cylinder was reheated again to ambient temperature and then weighed, and the mass of pentane was measured to be (2.660 ± 0.004) g. Methane was then added to give a total sample mass of (31.245 ± 0.004) g. Mixing was accomplished by shaking manually for ten minutes. Accounting for source fluid impurities and any potential unmixed dead volume in the valve, the overall mole fraction of the mixture was calculated as $z_2 = 0.0203 \pm 0.0003$.

This cylinder was connected to the equilibrium cell, and the connecting lines were evacuated and flushed several times with the mixture. A sample of the gas mixture was transferred to the equilibrium cell at a pressure of about 11 MPa, and the system was allowed to equilibrate at 293 K, a temperature above the mixture's cricondentherm calculated with the GERG-2004 XT08 EOS as being 285 K. Samples of the single-phase mixture were taken from both sampling lines (vapor and liquid) and analyzed using the FIDs' response ratios listed in Table 1. The difference in z_2 between the samples measured from the top and bottom was 0.0002, and the average was $z_2 = 0.0187 \pm 0.0007$ where the uncertainty bound includes the calibration uncertainties and the repeatability of about 15 measurements. The difference between the z_2 values determined from the gravimetric preparation and the GC measurement is about twice the combined uncertainties.

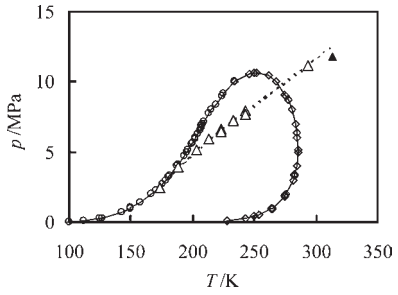

Figure 4. Pressures and temperatures of the VLE measurements relative to the phase envelope of the methane (1) + pentane (2) mixture with the overall mole fraction z_2 = 0.02 calculated using the GERG-2004 XT08 EOS. —○—, EOS bubble curve; —◊—, EOS dew curve; △, measured isochore points (including starting, single-phase point); ▲, last point measured on the isochore.

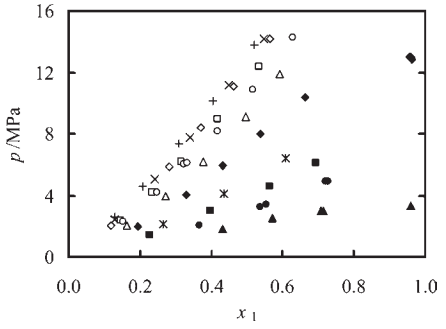

Figure 5. Pressures and liquid mole fractions x_1 measured for methane (1) + hexane (3) at 11 isotherms: ▲, 183 K; ●, 193 K; ■, 203 K; ∗, 213 K; ♦, 233 K; △, 253 K; ○, 273 K; □, 288 K; ◊, 303 K; ×, 318 K; +, 333 K.

This might be indicative of a problem with our techniques for preparing or transferring gas mixtures with small amounts of heavy components. However, the overall composition of the mixture in the cell is only used to plan VLE experiments and does not influence the phase composition measurements.

At 293 K and 11.13 MPa, the molar density of the mixture was calculated with the GERG-2004 XT08 EOS as 5.713 mol·dm^{-3}, and based on the equilibrium cell volume, the number of moles of mixture in the cell was estimated as 0.35 mol. The isochoric path for this constant molar density is shown in Figure 4, plotted at the same temperatures of our measurements, along with the phase envelope calculated with the GERG-2004 XT08 EOS.

The first value measured in the two-phase region was at 243 K, and then further measurements were taken every 10 K down to 173 K. Temperature was then increased, repeating measurements at (233 and 243) K. After finishing the measurements in the two-phase region, the cell temperature was increased to 313 K where the equilibrium pressure was measured as 12.49 MPa as shown in Figure 4 by the solid symbol. The average (single-phase) pentane mole fraction in the cell was z_2 = 0.0135 with a difference of 0.0007 between the top and bottom samples. The final pressure and composition measured at the end of the run indicated that the number of moles of the mixture decreased by about 0.02 mol in 0.35 mol, which agrees reasonably with about 100 injections daily of an average of $5 \cdot 10^{-7}$ mol, at a GC injector split ratio of 10, for 40 days.

For the methane + hexane system, measurements were made along 11 isotherms from (183 to 333) K, at pressures up to 14 MPa. The cell was first evacuated and flushed several times with pure methane, and then, while filled with methane at ≈0.2 MPa, approximately 5 mL of liquid hexane was pumped into the cell using an HPLC pump. To ensure the hexane in the cell was degassed, the system was heated to 333 K, and the valve to the vacuum pump was opened, while the stirrer was running. After the degassing was completed, the cell was then held at the desired temperature while methane gas was added to achieve the target pressure, and once the sample was mixed and reached equilibrium, the compositions for both the gas and liquid phases were measured. The next measurement at a different pressure, on the same isotherm, was then taken by either adding pure methane or venting the vapor phase of the mixture in the cell. Figure 5 shows the pressures at which our data were measured at different isotherms. The isotherm sequence was as follows: starting at 273 K the temperature was reduced five times to the lowest temperature of 183 K before being increased to 333 K and then repeating the measurements at 273 K. The average absolute standard deviation (AAD) of measurements was calculated as ± 0.002 for the range of liquid mole fractions of (0.12 to 0.96) and ± 0.0002 for the range of vapor mole fractions of (0.0002 to 0.0365). The most important observation in these measurements, as shown in Figure 5, is that significant methane mole fractions (> 0.95) were observed in the liquid phase for the maximum cell pressures on the (233 and 183) K isotherms.

RESULTS AND DISCUSSION

The results for methane (1) + pentane (2) are listed in Table 2 and for methane (1) + hexane (3) in Table 3. The temperatures listed in Table 2 are the average of the bottom and lid thermometers of the cell with the uncertainties obtained by combining in quadrature uncertainties arising from the temperature gradient along the cell, the standard deviation of the temperature over the course of the measurement, and the uncertainty of the PRT calibrations. The maximum combined uncertainty in the temperatures listed in Table 1 was $u_c(T) \approx 0.3$ K. However, the uncertainties in the temperatures for the methane + hexane are not listed in Table 3 because it had a much smaller value of $u_c(T) \approx 0.05$ K. This was because the additional thermal control, fitted to the cell top, reduced the thermal gradient along the cell to < 0.02 K.

For pressure, the relative standard uncertainty was ± 0.5 % of the reading in the range from (1 to 14) MPa, provided the temperature was within the range from (150 to 333) K. The pressure uncertainty was calculated from the quadrature combination of the standard deviation of the Kulite transducer's calibration with the standard deviation of the pressure measurement and had a maximum value of $u(p) \approx 0.04$ MPa for methane + pentane at the maximum pressure of 8 MPa and $u(p) \approx 0.07$ MPa for methane + hexane at the maximum pressure of 14 MPa.

The uncertainties in the composition measurements for the liquid phase $u(x_1)$ and for the vapor phase $u(y_i)$, listed in Tables 2 and 3, are the quadrature combination of the standard deviation in measurements and the contribution of the uncertainty of the ratio of the FID response coefficients (κ_i/κ_1) listed in Table 1. Generally, in analogy with Figure 3, the calibration uncertainty was the dominant contribution to $u(x_1)$ and $u(y_i)$; however, for some measurements the standard deviations of the measured areas (A_i/A_1) were the larger contribution. The maximum values of $u(x_1)$ and $u(y_i)$ are 0.005 and 0.0003 for methane + pentane and 0.013 and 0.0015 for methane + hexane, respectively. These

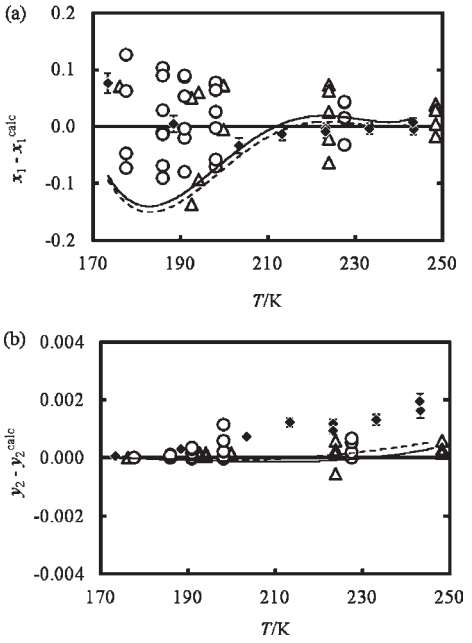

Figure 6. Deviations of measured mole fractions from those calculated with the GERG-2004 XT08 EOS at the measured pressure for methane (1) + pentane (2): (a) deviations in methane mole fraction x_1 in the liquid phase and (b) deviations in pentane mole fraction y_2 in the vapor phase. ♦, this work with error bars correspond to the values of $u_c(x_1)$ and $u_c(y_2)$ in Table 2; △, experimental data of Kahre;[12] ○, experimental data of Chu et al;[13] —, Peng−Robinson EOS (as implemented in ref 4) at the same T and p as this work; ---, advanced Peng−Robinson EOS[7] at the same T and p as this work.

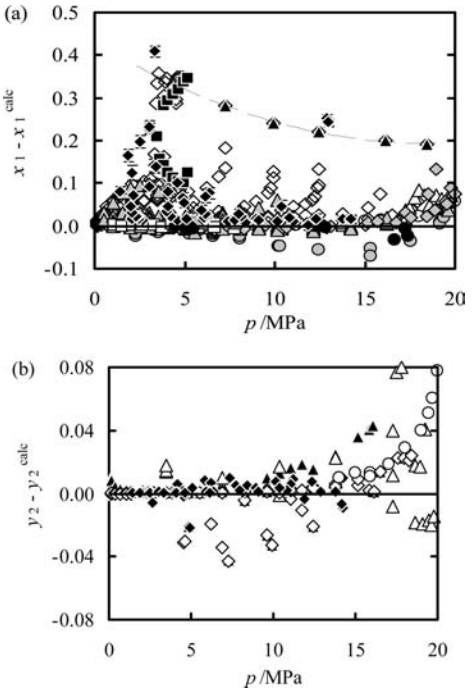

Figure 7. Differences between the measured mole fractions from those calculated with the GERG-2004 XT08 EOS for methane (1) + hexane (3): (a) differences in the liquid mole fraction x_1 and (b) differences in vapor mole fraction y_3: ♦, this work; gray-filled triangle, ref 14; ◊, ref 15; gray-filled diamond, ref 16; △, ref 17; ●, ref 19; □, ref 21; ○, ref 22; gray-filled circle, ref 24; ▲, ref 10; ■, ref 11; - - -, second liquid phase reported by Chen et al.[10] and Merrill et al.[11]

uncertainties are independent of the uncertainties propagated from temperature and pressure measurements and merely represent the repeatability of sampling and the accuracy of the GC analysis. The combined uncertainties $u_c(x_1)$ and $u_c(y_i)$ were obtained by combining in quadrature the uncertainties propagated from the temperature and pressure calculated with the GERG-2004 XT08 EOS and the uncertainties $u(x_1)$ and $u(y_i)$, respectively. For the methane + pentane measurements, the propagated uncertainty in the liquid mole fractions arising from temperature $u(x_1)_T$ had a value of 0.0016 at 243 K and 7.6 MPa, while at 173 K and 2.4 MPa, the lowest point on the isochore, it had a value of 0.016 which is ten times higher. Similarly, the composition uncertainty arising from pressure, $u(x_1)_p$, increased from 0.004 at 243 K and 7.6 MPa to 0.007 which is about two times higher at the lowest point of 173 K and 2.4 MPa. For the methane + hexane measurements, the propagated uncertainty in the liquid mole fractions was smaller, mainly because the uncertainty in temperature measurements was ten times lower than for the methane + pentane measurements. For the combined uncertainties in the vapor phase mole fractions $u_c(y_i)$, the contributions propagated from the temperature and pressure uncertainties were negligible compared to the uncertainties in the GC composition measurements $u(y_i)$ as shown in Tables 2 and 3.

The measured vapor-phase mole fractions of the heavy component y_i were from $(1 \text{ to } 98)\cdot 10^{-4}$ for the pentane, as listed in Table 2, and $(2 \text{ to } 390)\cdot 10^{-4}$ for the hexane as listed in Table 3. Thus, the combined relative uncertainty in some of these measurements (usually $y_i < 0.001$) was as high as 150 % of the measured value. For the liquid-phase mole fractions, the relative uncertainties were generally about 2 % in the measured range of x_1 from (0.5 to 0.99) for methane (1) + pentane (2) and from (0.12 to 0.96) for methane (1) + hexane (3).

At three conditions across the two mixtures, corresponding to extremes of low temperature and/or high pressure, the mole fraction of methane in the liquid phase increased considerably to $x_1 > 0.95$, and although our cell was not designed to measure more than one liquid phase, we presume that in these cases a second liquid phase rich in methane was formed in the region from which the liquid capillary sampled. In methane (1) + hexane (3), at 183 K and 3.3 MPa, and at 233 K and 13 MPa, x_1 was measured as ≈0.955 with a good agreement with the three phase VLLE measurements reported by other workers[10,11] as shown in Figure 7a. The GERG-2004 XT08 EOS failed to predict the second liquid phase, and although the PR and APR EOS are capable of calculating a second liquid phase, all three EOS predicted one liquid phase with $x_1 \approx 0.7$ at these conditions

For methane (1) + pentane (2), our measurement of $x_1 = 0.99$ at 173 K and 2.4 MPa, which is 3 K lower than any previous liquid measurement reported in the literature, is somewhat anomalous in comparison with the rest of the data. At this condition the GERG-2004 XT08 EOS predicts a value of 0.92, while the PR and APR EOS both predict a value of 0.83. Unlike methane + hexane, no second liquid phase has been reported in the literature for methane + pentane; however, Kahre[12] did observe a distinct inflection on the p,x curve at low temperatures and high pressure for binary mixtures of methane with propane, butane, and pentane and concluded that the inflection in the p,x curve increases (curve becomes more horizontal) with increasing carbon number of the heavy component. Kahre[12] conjectured that this

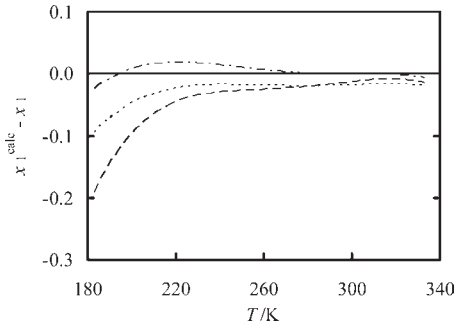

Figure 8. Differences between the measured mole fractions in the liquid phase x_1 for methane (1) + hexane (3) from those calculated with an EOS, x_1^{calc}, at the same temperatures and pressures listed in Table 2 {excluding the values at 183 K, 3.3 MPa and 233 K, 13 MPa}: · · · · ·, Peng−Robinson EOS (as implemented in ref 4); - · - · -, advanced Peng−Robinson EOS;[7] - - -, GERG-2004 XT 08 EOS.[6]

inflection could eventually result in a phase separation, and it is therefore possible that in our measurement at 173 K and 2.4 MPa that our sample came from a second liquid phase of the methane + pentane mixture.

The differences between the experimental mole fractions, listed in Table 2, and those calculated using the GERG-2004 EOS for the methane (1) + pentane (2) are shown as a function of temperature in Figure 6a for the liquid phase $(x_1 - x_1^{calc})$ and in Figure 6b for the vapor phase $(y_2 - y_2^{calc})$, where the superscript calc denotes the mole fraction calculated with the GERG-2004 XT08 EOS at the experimental pressure and temperature. The uncertainty bars shown in Figure 6 correspond to the values of $u_c(x_1)$ and $u_c(y_2)$ in Table 2. Selected literature data from Kahre[12] and Chu et al.[13] are included, and the differences for the liquid phase mole fractions measured in this work (Figure 6a) are about 0.01 at the higher temperatures and increase at lower temperatures to about 0.1 at x_1 = 0.99. The differences shown in Figure 6a for the other experimental data are similar but also show an increase with pressure. The difference curves for values of x_1 calculated with the PR and APR EOS at the temperature and pressure listed in Table 2 are also shown in Figure 6. At temperatures above 210 K, all three EOS are in good agreement with the current measurements. At 203 K, the two cubic EOS remain in agreement with the value measured here, while the GERG-2004 XT08 EOS prediction is larger by nearly 0.04. However at 188 K the situation reverses with the cubic EOS underpredicting the value of x_1 by nearly more than 0.1. For the vapor phase mole fractions, shown in Figure 6b, the predictions of all three EOS are very similar and are consistent with the data within the experimental uncertainty, although there is an indication that the cubic EOS match the data's trend with temperature slightly better than the GERG-2004 XT08 EOS.

There is extensive literature data[14−25] reported for methane + hexane from (138 to 444) K and at pressures from (0.12 to 20) MPa. The differences between (i) literature data and (ii) our experimental data listed in Table 3 from those calculated with GERG-2004 XT08 EOS (represented by the zero line) are shown in Figure 7a for the liquid phase $(x_1 - x_1^{calc})$ and Figure 7b for the vapor phase $(y_3 - y_3^{calc})$. The systematic increase in the differences from the GERG-2004 EOS with pressure at constant temperature shown in Figure 7a is clear evidence that the equation needs refinement to account for high-pressure effects and the presence of a second liquid phase. Our liquid-phase data agree well with literature values, and the second liquid-phase data measured at 183 K and 3.3 MPa and at 233 K and 13 MPa lie within the second liquid-phase results reported by Chen et al.[10] and the two liquid phases reported by Merrill et al.[11] The differences in the vapor-phase mole fraction had an average of 0.01 as shown in Figure 7b and with the increase in the temperature and pressure.

For clarity, the differences between our data x_1 from those calculated x_1^{calc} with the PR and APR EOS are not included in Figure 7a but are shown in Figure 8, along with those calculated with the GERG-2004 XT08 EOS at the same temperatures and pressures listed in Table 3. At the lowest temperature of 183 K, the differences $(x_1 - x_1^{calc})$ were ≈0.25 using the GERG-2004 EOS, ≈0.15 using the PR EOS, and ≈0.05 using the APR EOS. The APR EOS appears to perform better than the PR EOS and GERG-2004 XT08 EOS in predicting x_1 for the methane + hexane mixture.

AUTHOR INFORMATION

Corresponding Author

*E-mail: eric.may@uwa.edu.au.

Funding Sources

The research was funded by Chevron Energy Technology Company, the Western Australian Energy Research Alliance, and the Australian Research Council. One of us (M.J.T.) was supported as an exchange student by the Technical University of Munich, Germany.

ACKNOWLEDGMENT

The authors thank Craig Grimm for helping to construct and maintain the apparatus. The authors are also grateful to Jeff Buckles for his contributions to the project.

REFERENCES

(1) Laskowski, L; Kandil, M. E.; May, E. F.; Trebble, M. A.; Trengove, R. D.; Trinter, J.; Huang, S.; Marsh, K. N. AIChE Spring Meeting, April 2008, 8th Topical Conference on Natural Gas Utilization, New Orleans, LA, April 6−10, 2008.

(2) Peng, D. Y.; Robinson, D. B. A New Two Constant Equation of State. *Ind. Eng. Chem. Fundam.* **1976**, *15*, 59–64.

(3) Soave, G. Equilibrium Constants from a Modified Redlich-Kwong Equation of State. *Chem. Eng. Sci.* **1972**, *27*, 1197–1203.

(4) *Aspen HYSYS Process Simulator*, v7.1; Aspen Technology, Inc.: Cambridge, MA, 2009.

(5) *HYSYS 2004 Simulation Basis*, p A-5; Aspen Technology: Cambridge MA, 2004.

(6) Kunz, O.; Klimeck, R.; Wagner, W.; Jaeschke, M. *The GERG-2004 Wide-Range Equation of State for Natural Gases and Other Mixtures*, GERG Technical Monograph 15, 2007, Fortschr.-Ber. VDI, Reihe 6, Nr. 557, VDI Verlag, Düsseldorf.

(7) *VMGSim Process Simulator*, v5.0.5; Virtual Materials Group, Inc., 2002−2009.

(8) Kandil, M. E.; May, E. F.; Graham, B. F.; Marsh, K. N.; Trebble, M. A.; Trengove, R. D.; Huang, S. H. Vapor-Liquid Equilibria Measurements of Methane + 2-Methylpropane (Isobutane) at Temperatures from (150 to 250) K and Pressures to 9 MPa. *J. Chem. Eng. Data* **2010**, *55*, 2725–2731.

(9) Dietz, W. A. Response Factors for Gas Chromatographic Analyses. *J. Gas Chromatogr.* **1967**, *5*, 68–71.

(10) Chen, R. J. J.; Chappelear, P. S.; Kobayashi, R. Dew-Point Loci for Methane-n-Hexane and Methane-n-Heptane Binary Systems. *J. Chem. Eng. Data* **1976**, *21*, 213–219.

(11) Merrill, R. C.; Luks, K. D.; Kohn, J. P. Three-phase Liquid-Liquid-Vapor Equilibria in the Methane + n-Pentane + n-Octane, Methane + Hexane + n-Octane, and Methane + n-Hexane + Carbon Dioxide Systems. *J. Chem. Eng. Data* **1983**, *28*, 210–215.

(12) Kahre, L. C. Low-Temperature K Data for Methane-n-Pentane. *J. Chem. Eng. Data* **1975**, *20*, 363–367.

(13) Chu, T.; Chen, R. J. J.; Chappelear, P. S.; Kobayashi, R. Vapor-Liquid Equilibrium of Methane-n-Pentane System at Low Temperatures and High Pressures. *J. Chem. Eng. Data* **1976**, *21*, 41–44.

(14) Shim, J.; Kohn, J. P. Multiphase and Volumetric Equilibria of Methane + *n*-Hexane Binary System at Temperatures Between −110 and 150 °C. *J. Chem. Eng. Data* **1962**, *7*, 3–8.

(15) Lin, Y. -N.; Chen, R. J. J.; Chappelear, P. S.; Kobayashi, R. Vapor-Liquid Equilibrium of the Methane-*n*-Hexane System. *J. Chem. Eng. Data* **1977**, *22*, 402–408.

(16) Schoch, E. P.; Hoffmann, A. E.; Mayfield, F. D. Solubility of Methane in Hexane. *Ind. Eng. Chem.* **1941**, *33*, 688–691.

(17) Poston, R. S.; McKetta, J. J. Vapor-Liquid Equilibrium in the Methane-n-Hexane System. *J. Chem. Eng. Data* **1966**, *11*, 362–363.

(18) Chylinski, K.; Djamarani, K.; Drummond, I. W.; Saville, G.; Wakeham, W. A. Phase Equilibrium Measurements in Gas-condensates. *Fluid Phase Equilib.* **1992**, *76*, 225–235.

(19) Sage, B. H.; Webster, D. C.; Lacey, W. N. Phase Equilibria in Hydrocarbon systems. XVI. Solubility of Methane in Four Light Hydrocarbons. *Ind. Eng. Chem.* **1936**, *28*, 1045–1047.

(20) Stepanova, G. S.; Vybornova, Ya. I. Phase equilibriums of methane-hexane system. From Tr. Vses. Nauchn-Issled. *Inst. Priorodn. Gazov.* **1962**, 203–8.

(21) Srivastan, S.; Darwish, N. A.; Gasem, K. A. M.; Robinson, R. L. Solubility of Methane in Hexane, Decane, and Dodecane at Temperatures from 311 to 423 K and Pressures to 10.4 MPa. *J. Chem. Eng. Data* **1992**, *37*, 516–520.

(22) Marteau, P.; Obriot, J.; Barreau, A.; Ruffier-Meray, V.; Behar, E. Experimental Determination of the Phase Behavior of Binary Mixtures: Methane-Hexane and Methane-Benzene. *Fluid Phase Equilib.* **1997**, *129*, 285–305.

(23) Gunn, R. D.; McKetta, J. J.; Ata, N. Measurement and Prediction of High-pressure Phase Equilibria with a Dilute Component in the Gas Phase: The Methane-n-Hexane System. *AIChE J.* **1974**, *20*, 347–353.

(24) Cebola, M. J.; Saville, G.; Wakeham, W. A. VLE Measurements at High Pressures and High Temperatures on (Methane + n-Hexane). *J. Chem. Thermodyn.* **2000**, *32*, 1265–1284.

(25) Luks, K. D.; Hottovy, J. D.; Kohn, J. P. Three-Phase Solid-Liquid-Vapor Equilibria in the Binary Hydrocarbon Systems Methane-n-Hexane and Methane-Benzene. *J. Chem. Eng. Data* **1981**, *26*, 402–403.